Journal of the European Ceramic Society 23 (2003) 935–942

www.elsevier.com/locate/jeurceramsoc

Co-extrusion of Al_2O_3/ZrO_2 bi-phase high temperature ceramics with fine scale aligned microstructures

C. Kaya[a,*], E.G. Butler[a], M.H. Lewis[b]

[a]*Interdisciplinary Research Centre (IRC) in Materials Processing and School of Metallurgy and Materials, The University of Birmingham, Edgbaston, Birmingham, B15 2TT, UK*

[b]*Department of Physics, Centre for Advanced Materials, University of Warwick, Coventry, CV4 7AL, UK*

Received 1 March 2002; received in revised form 24 June 2002; accepted 30 June 2002

Abstract

Structural ceramic composites comprising continuous fibrillar microstructure are produced using sol-based technology which involves the extrusion, at room temperature, of a two-phase material (Al_2O_3/ZrO_2) resulting in an aligned bi-phase structure which is then multiple co-extruded to reduce the lateral dimensions of the phases. Two sol-derived pastes of differing chemistry (γ-AlOOH as alumina source and zirconia) are co-extruded in parallel, and layed-up in closed-packed linear array to form a heterogeneous macro-plug for subsequent extrusion with or without zirconia coating. The second and third extrusion steps produce a filament with markedly reduced lateral paste dimensions provided that the flow properties of the chemically different pastes are similar. The resulting extrudates in the form of continuous green monofilaments, are subsequently laid up in a mould where the structure is pressed and consolidated in desired shape, then pressureless sintered in air to form the multi-phase component. The developed process allows the microstructure to be controlled at a nanometer scale within each extruded filament and after the 3rd stage co-extrusion, each filament size within the final extrudate is reduced to ≈ 65 μm.

Keywords: Aligned microstructure; Al_2O_3; Extrusion; Sol-gel processes; ZrO_2

1. Introduction

In the last two decades, new materials are required for lightweight rigid structures with potential for high temperature operation in the aerospace industry, as the most developed alloy systems have reached a development limit in relation to high temperature stability and deformation resistance. Monolithic ceramics can not be used for such applications due to their low fracture toughness and low resistance to thermal shock. Continuous fibre-reinforced ceramic matrix composites are the best solution for high-risk engineering components in which high specific stiffness and high temperature tolerance are required.[1–5] However, they are very expensive to fabricate and current available fibres are stable only up to 1200 °C.

Co-extrusion can be defined as the passing of two or more pastes through the same die to manufacture a green body of uniform cross sectional area. It has been widely used recently to produce multilayer ceramics,[6] multilayer tubes,[7] alumina and PbO-containing ferroic ceramics,[8] lead manganese niobate-lead titanate ceramics and silver palladium,[9] zirconia and stainless steel metal-ceramic pipes[10] and fine-scale alumina, mullite and ZTA components.[11–14] One of the main advantages of using a co-extrusion technique is the significant reductions in the number of processing steps. It has proven also that deliberately introduced weak interfaces in a laminar structure suppresses the catastrophic failure, increases the fracture toughness and work of fracture by the operation of debonding and crack deflecting mechanisms.[15]

The main objective of the present work is to demonstrate the feasibility of forming multiphase aligned fibrillar micostructures from nano-size sol particle precursors using an innovative multiple co-extrusion process. For this aim, two sol-derived high solids-loading

* Corresponding author. Tel.: +44-121-4143537; fax: +44-121-4143441.

E-mail address: c.kaya@bham.ac.uk (C. Kaya).

0955-2219/03/$ - see front matter © 2002 Elsevier Science Ltd. All rights reserved.
PII: S0955-2219(02)00227-3

pastes of alumina and zirconia are co-extruded in parallel, and layed-up in closed-packed linear array to form a heterogeneous macro-plug for subsequent extrusion provided that the flow properties of the chemically different pastes are similar.

2. Experimental work

2.1. Paste preparation from seeded boehmite (γ-AlOOH) sol

Boehmite (γ-AlOOH) sol (Remal A20, Remet corp., USA) was used as the alumina source. The sol has average particle size and solids-loading of 40 nm and 20 wt.%, respectively. The as received sol is stable at a pH value of 4. The received boehmite sol was seeded with 2 wt.% of the total mass using ultrafine α-Al_2O_3 (30 nm, BDH Chemical, UK., high purity polishing powder) powders. The flow chart for the seeding process, followed by paste preparation is given in Fig. 1. To seed the boehmite sol, the seeding powders was first dispersed in distilled water and then added into boehmite sol. Glycerol (1 wt.%) and celacol (1 wt.%) were also added in order to minimise the surface roughness of the extruded and increase the green strength, respectively. Celacol (1 wt.%) was first dissolved in water at 85 °C and then added to the seeded sol in order keep it plastically deformable during the multiple extrusion stage.

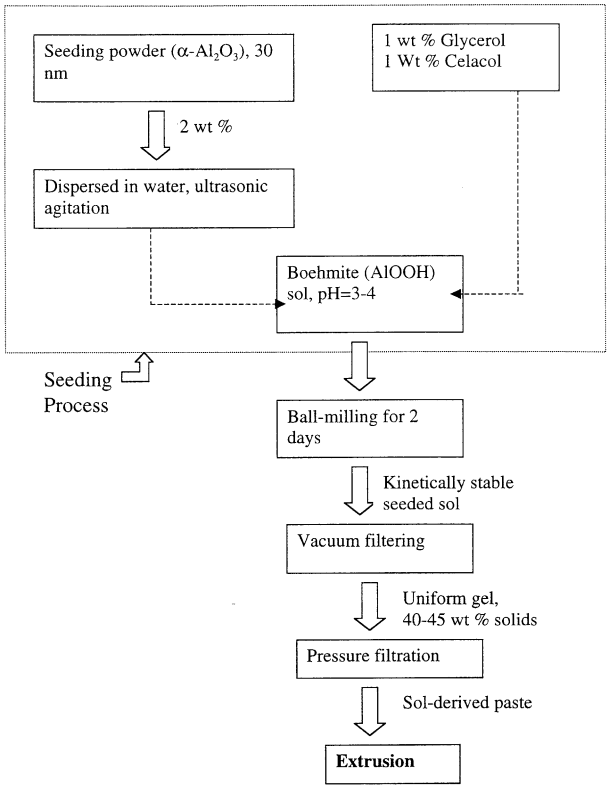

Fig. 1. Flow chart for the preparation of boehmite sol-derived paste.

The seeded sol was first stirred magnetically for 10 h and then ultrasonic agitation was employed at 15 kHz for 3 h for further dispersion of any particle agglomerates which might be present.[16] The final sol composition i.e., boehmite + 2 wt.% seeding powder + 1 wt.% glycerol + 1 wt.% celacol was ball-mixed for 2 days using high purity zirconia balls. Before and after ball-milling, the zirconia balls were weighted to ensure that there was no contamination resulting from the milling media. The mixed seeded sol was then vacuum filtered in order to obtain a gel structure. The resulting soft white gel was further compacted using pressure filtration apparatus to squeeze out the excess water, and obtain an extrudable paste.[17]

2.2. Zirconia sol-paste preparation

Zirconia sol was prepared using ultrafine and high purity zirconia powders (average grain size is 30 nm, VP zirconia, Degussa Ltd., Germany) with the addition of 3 mol% yttria. Kinetically stable and well dispersed zirconia sol having 20 wt.% solids-loading was prepared by the addition of small amount of zirconia to the water, while the suspension was magnetically stirred. The best pH value in order to obtain the maximum stability was found to be 8.5 and this pH value was maintained using ammonia. 1 wt.% glycerol and celacol were added to prepared zirconia sol. Cyclohexanone ($C_6H_{10}O$) (1 wt.%) and 1 wt.% boehmite sol were also added in order to minimise the shear-thickening effect. The flow chart for zirconia gel and paste preparation is given in Fig. 2. Each paste was then extruded using a laboratory scale extrusion apparatus with an extrusion reduction ratio of 4:1. The ram velocity chosen was very low (0.5 or 1 mm/min.) to minimise edge-tearing defects that might form at higher velocities. Flow behaviour of each paste was determined using a computer program linked to the Instron test machine. Rheological behaviour of each material, i.e., boehmite and zirconia was controlled to be similar for multiple extrusion.

2.3. Paste rheology

The rheological behaviour of boehmite and zirconia sol-derived pastes was characterised by a capillary rheometer.[18–20] Three dies with different L/D (length/diameter) ratios were used. The ram speeds ranged from 124 to 0.5 mm/min. and the load at each-pre-set velocity was recorded. The paste rheology was characterised using the Benbow–Bridgwater relationship:[21]

$$P = 2\mathrm{Ln}(D_o/D)(\sigma_o + \alpha_1 V^m) + 4(L/D)(\tau_o + \beta_1 V^m) \quad (1)$$

where P is the pressure, D_o and D are the diameters of the barrel and the die, respectively, L is the length of the die land and V is the extrudate velocity. The paste

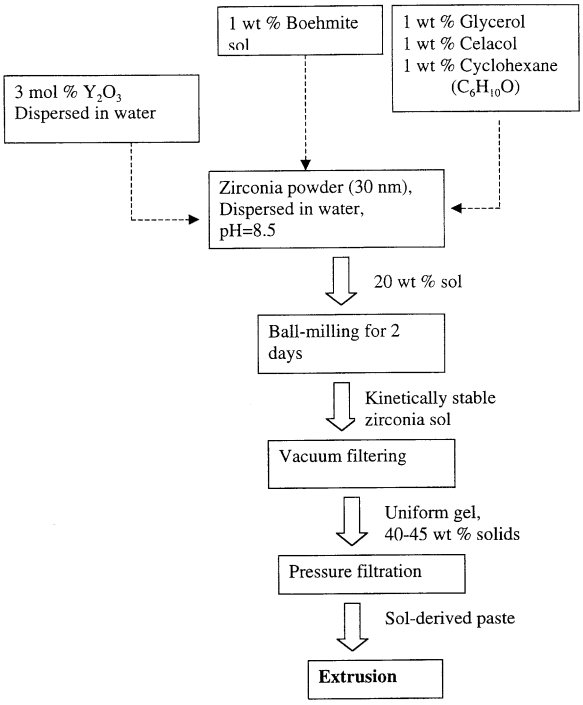

Fig. 2. Flow chart for the preparation of zirconia sol-derived paste.

parameters that describes the paste flow during extrusion are σ_o the die entry yield stress; τ_o the die wall shear stress; α, and β, the die entry and die land velocity coefficients. The m and n are the die entry and die land velocity exponents; these are used to describe non-linear pressure versus velocity data.

2.4. Multiphase green body formation by multiple co-extrusion

The flow chart for multiphase green body formation using multiple co-extrusion, is shown in Fig. 3. As shown in the monofilament extrusion section, square shaped (4×4 mm) boehmite and zirconia monofilaments were first extruded separately. Then a total of 16 monofilaments (8 boehmite and 8 zirconia) were un-coated or dip coated with zirconia before they are layed-up in a square die. After the first co-extrusion, each co-extruded filament included 16 filaments and filament size was reduced from 4 to 1 mm using a 4 mm square die.[22] For the second co-extrusion, the same process was repeated and the twice co-extruded filament included 256 monofilaments (128 boehmite and 128 alumina) having a filament size of 250 μm. After the third stage co-extrusion, each extruded filament contained 4096 filaments and a filament size of 62.5 μm. During each step of this process, a zirconia interface was applied, using dip coating. Manufacture of the multiphase consolidated test plaques with zirconia interfaces using die pressing was carried out, as shown in the multiphase green body formation section in Fig. 3. For this aim, 3rd stage co-extruded boehmite/zirconia filaments were first produced with zirconia interface. These multiple co-extruded and plastically deformable zirconia coated filaments were layered (two or three multiple co-extruded filaments in each layer) in a rectangular die ($70\times12\times50$ mm^3) and then pressed using an applied load of 10 kN. If two layers of multiple co-extruded filaments were pressed in the die, the final test plaque contained 24 546 filaments whilst in the case of three layers, the number of filaments within the test plaque was 36 864.

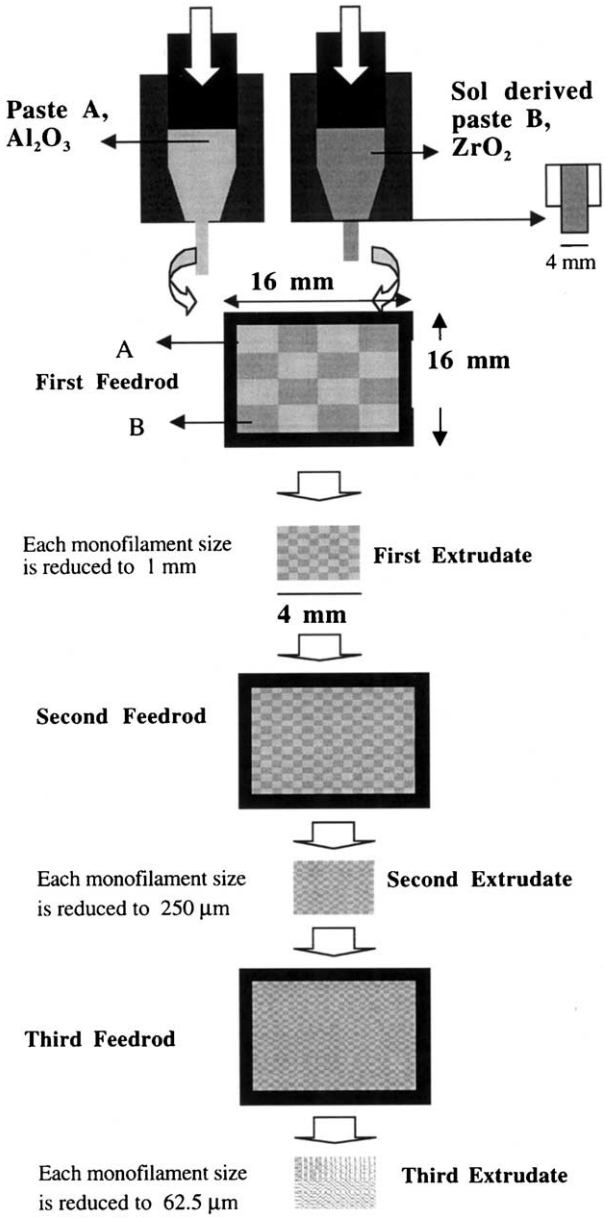

Fig. 3. Schematic representation of multiphase component fabrication by multiple co-extrusion.

2.5. Monofilament coating with ZrO_2

In order to prepare a low solids-loading zirconia suspension suitable for coating, Degussa zirconia powders

(VP zirconia, 30 nm) were dispersed in distilled water. Kinetically stable, well dispersed zirconia suspensions containing 5–10 wt.% zirconia powders were obtained at a pH value of 3. Then, the green extrudates were immersed in an ammonia based solution, consisting of an ammonium salt of polymethacrylic acid (Versicol KA21, pH: 9, Allied Colloids, UK and Versicol E10) adjusted by pure ammonia solution to pH 11.5, thus creating a negative surface charge and improving the wetting of the extrudates surface. This stage maximised the electrostatic attraction between the extrudates surface and the positively charged zirconia particles in the coating sol (see Fig. 4).

2.6. Drying and sintering

The consolidated multiphase green samples, i.e., multiple extruded and pressed, were first kept in a humidity controlled chamber (from 80 to 55% relative humidity) for 1 day to allow the residual water to remove slowly from the green body, thus preventing the formation of any internal cracks. This was followed by 1 day drying in normal air. The dried green body compacts were pressureless sintered at 1400 °C for 2 h in air using a 3 °C/min. heating and cooling rates (the green samples were first heated to 110 °C using a 2 °C/min. heating rate for 2 h, then 600 °C using 3 °C/min. heating rate for 2 h in order to burn out any residual organic materials that might be present within the body).

2.7. Other characterisation techniques

Microstructural examinations on green and sintered samples were carried out using a Field Emission Gun SEM (FEG SEM FX-4000, Jeol Ltd. Japan) and sintered densities were measured using Archimedes technique. Interface behaviour in terms of the crack deflection/arrest was characterised using a crack propagation test.[23,24] A linear intercept technique was used to measure the average grain size on polished and thermally etched surfaces.[25]

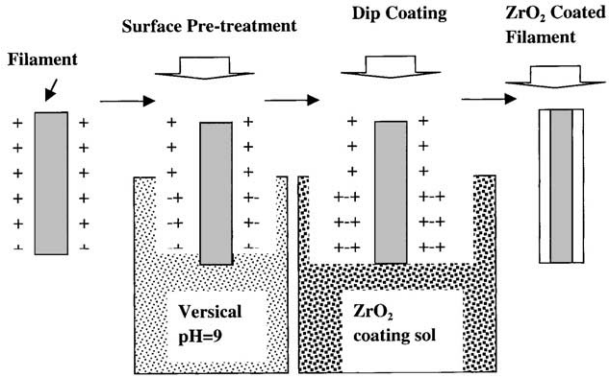

Fig. 4. Schematic representation of dip-coating technique.

3. Results and discussion

Fig. 5 shows the flow behaviour of the chemically different boehmite and zirconia pastes during monofilament extrusion using a constant speed of 0.5 mm/min. The success of the multiple extrusion relies on the rheology of the two pastes being matched. The sol-derived boehmite and zirconia pastes (see Figs. 1 and 2) show similar rheological behaviour, as shown in Fig. 5. If one paste is softer than the other, the resultant differences in velocities cause the formation of non-discrete shapes. The phenomenon of phase migration occurs when the water flows preferentially through the powder system under an applied stress.[18] If phase migration takes place during extrusion (due to unwell mixture of each of the constituents within the paste or extrusion at low deformation rates etc.) the load at each ram speed can not be accurately determined. Boehmite and zirconia sol-derived pastes display a very stable paste flow behaviour as shown in the load-distance curves in Fig. 5.

The shear stress versus shear rate curves for boehmite and zirconia pastes (for a constant L/D: 16) are shown in Fig. 6(a). As shown in Fig. 6(a) the gradient of the curves decrease as the shear rate increases, indicating that both pastes are shear thinning and can be co-extruded using similar extrusion parameters. The rheology of the pastes can be described as non-Newtonian Herschel–Bulkley flow which follows a power law function indicating the existance of a critical yield stress which must be exceeded for flow to occur.[26] Measured pressure drops as a function of extrusion velocity for a constant L/D: 16 for boehmite and zirconia sol-derived pastes are shown in Fig. 6(b) confirming the presence of very similar flow behaviour of the pastes. The rheological behaviour of ceramic pastes is mainly determined by the powder size, morphology, size distribution, powder loading and binder rheology.[19] As explained in Figs. 1

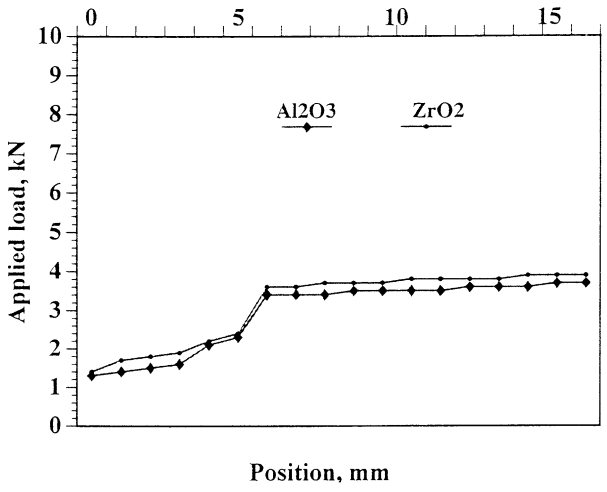

Fig. 5. Load-distance curves of boehmite and zirconia during monofilament extrusion.

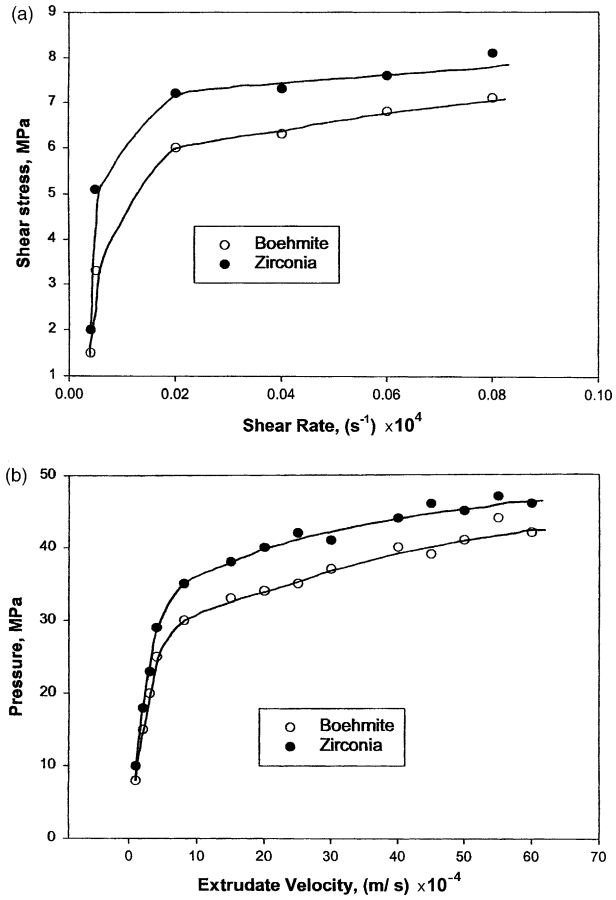

Fig. 6. (a) Shear stress–shear rate and (b) measured pressure changes as a function of extrudate velocity for a constant L/D: 16 for boehmite and zirconia sol-derived pastes.

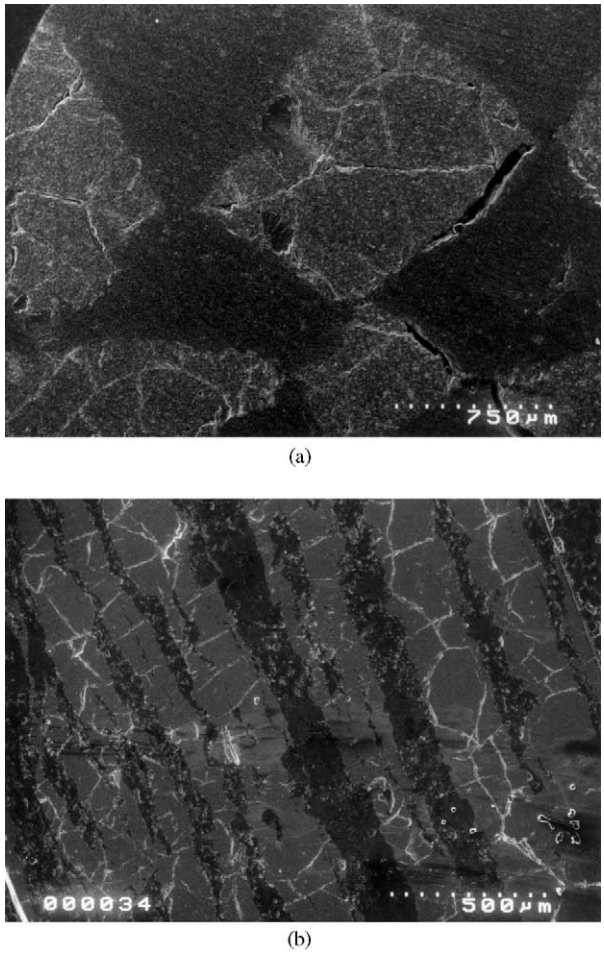

Fig. 7. SEM images of co-extruded boehmite/zirconia multiphase component, showing the presence of cracks within the zirconia phase (light phase) if the rheological behaviour of two pastes are not similar and the difference in sintering shrinkage is about 7%. (a) cross sectional and (b) longitudinal view (sample was sintered at 1400 °C for 2 h.).

and 2, both pastes used in this work are water based and contains very small amount of additives as binder or solvent, therefore, it can be concluded that the rheological behaviour of each paste is dependant on the particle characteristics such as size, shape and loading as well as the chosen processing technique. of the pastes. The developed technique for the preparation of sol-derived pastes provides homogeneously mixed pastes suitable for co-extrusion under the same extrusion parameters. Otherwise, it is not possible to prepare a paste from nano-size particles using conventional paste preparation techniques.

The other critical parameter is the drying behaviour of the pastes. Fig. 7(a) shows a cross-sectional SEM micrograph, indicating the effect of the rheology matching of the two pastes on the microstructure of co-extruded component. For successful co-extrusion, both rheology, the drying and the sintering shrinkage of the pastes should be controlled in order to control the internal stresses and cracking. Fig. 7(a) shows a 1st stage co-extruded alumina/zirconia microstructure after sintering at 1400 °C for 2 h. Significant crack formation is visible within the zirconia phase (light phase) also at the interface when zirconia shows "shear thickening" behaviour during extrusion and the difference in linear sintering shrinkage between these two phases is about 7% as shown in Fig. 7(a). The presence of extensive cracks (caused by the difference in sintering shrinkage) perpendicular to the extrusion direction within the zirconia filaments is also evident from the longiditunal section of co-extruded sintered filament shown in Fig. 7(b). If the right rheology, drying cycle and sintering shrinkage are optimised using the necessary additions (see Figs. 1 and 2), crack free co-extruded filaments are produced as shown in Fig. 8. Fig. 8(a) and (b) show the cross-sectional and longidutional microstructure of a 2nd stage co-extruded alumina/zirconia biphase filament after sintering at 1400 °C for 2 h. In order to optimise the linear sintering shrinkage of zirconia, 2 wt.% coarse zirconia powders (300 nm) were added to the main composition as described in Fig. 2, so that the difference in sintering shrinkage between these two phases is controlled to be less than 3%. Crack formation within

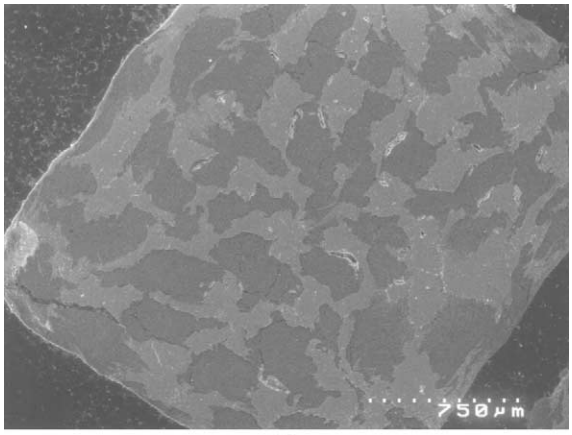

(a)

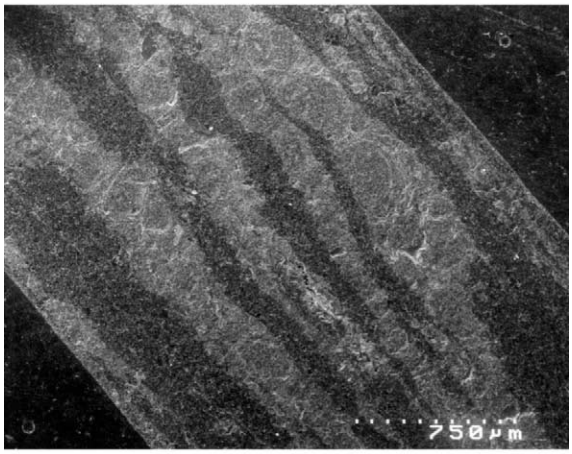

(b)

Fig. 8. SEM images of co-extruded boehmite/zirconia multiphase component, showing the absence of cracks within the phases or at the interface if the rheological behaviour of two pastes is controlled to be similar and the difference in sintering shrinkage is $<3\%$. (a) cross sectional and (b) longitudinal view (sample was sintered at 1400 °C for 2 h).

the any phase or at the interface is avoided, as shown in Fig. 8(a) and (b). It should also be noted from Fig. 8 that there is a shape distortion in alumina and zirconia due to difference in water removal behaviour of the pastes during extrusion as they have different particle shapes and packing densities in the paste form. However, this is considered not to be a critical issue providing the each filament within the co-extruded structure is continuous.

Fig. 9 demonstrates a 3rd stage co-extruded alumina/zirconia microstructure with the absence of any inter or intragranular porosity as well as cracks after sintering at 1400 °C for 2 h. One of the main objectives of the present work is to control the fine-scale sintered microstructure of the each phase present in the final sintered component using ultrafine starting powders (<100 nm). Fig. 9 shows the very fine and dense microstructures of zirconia (in TZP form by the addition of 3 mol% Y_2O_3) and α-alumina after sintering at 1400 °C for 2 h. The

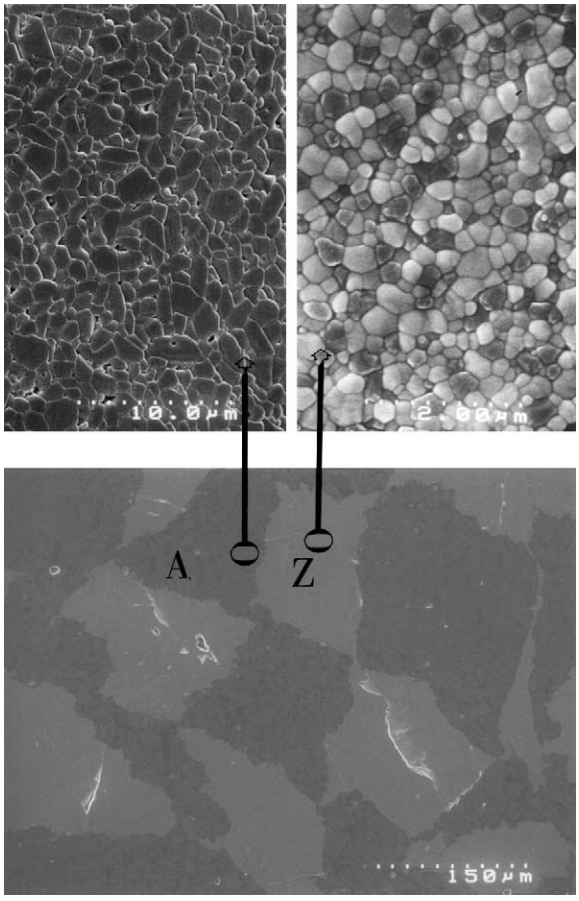

Fig. 9. SEM images of 3rd stage co-extruded alumina/zirconia component, showing the fine microstructure of zirconia phase and dense microstructure of α-alumina (A: α-alumina, Z: zirconia). Sample sintered at 1400 °C for 2 h.

average grain size of alumina and zirconia within the co-extruded and sintered bi-phase component was determined to be 1.6 and 0.45 μm, respectively. The zirconia microstructure contains only equiaxed grains whilst the majority of grains in the alumina matrix are near equiaxed with the presence of some elongated ones, as shown in Fig. 9. These fine scale microstructures are expected to provide good mechanical and thermo-mechanical properties. Figs. 7–9 show the microstructural features in assessing the effectiveness of the co-extrusion technique in order to produce di-phasic aligned microstructures and it can be concluded from these micrographs that the rheological matching of the two different pastes coupled with differential sintering shrinkage's play the most critical role for a successful co-extrusion. Shape distortion of each filament during co-extrusion is also noted as shown in Figs. 8 and 9. This distortion in shape can be eliminated using lower extrusion reduction ratios or extrusion rates.

The microstructures of zirconia coated monofilament using dip-coating are shown in Fig. 10. Homogeneous coating around an alumina rod in green state is evident from the micrograph shown Fig. 10(a) and its thickness

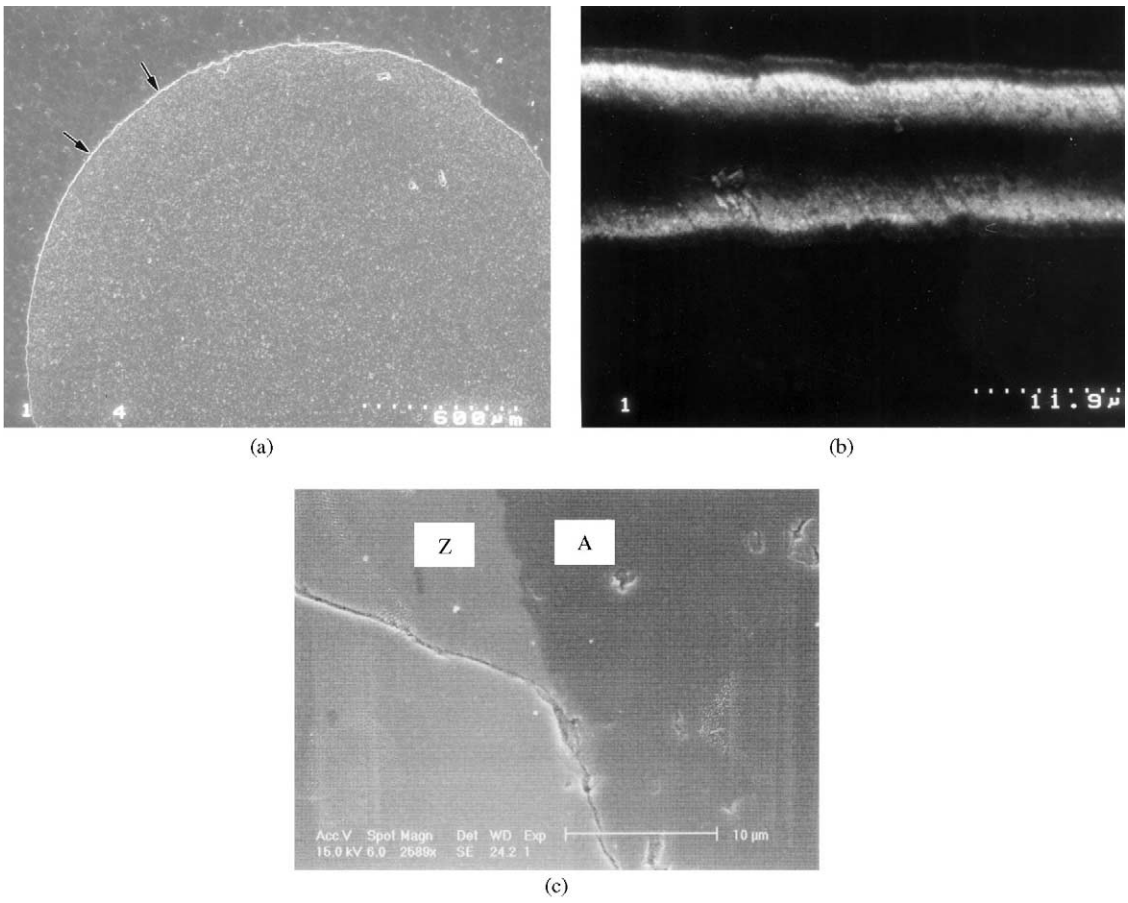

Fig. 10. SEM images of a zirconia coated monofilament, showing (a) the homogeneous zirconia layer around the filament, (b) the thickness of the zirconia layer to be about 10 μm and (c) the propagation of an indenter-induced crack at the alumina/zirconia interface (A: alumina and Z: zirconia).

is about 10 μm as shown in Fig. 10(b). These pictures clearly show the effectiveness of the dip-coating process which relies on the strong electrostatic attraction between the coating sol particles and extrudate surface. The propagation of an indenter induced crack on a co-extruded filament with zirconia interface is shown in Fig. 10(c). It is shown that the zirconia interface created between alumina and zirconia phases within the co-extruded filament is able to deflect the crack along the boundary.

4. Conclusions

This work introduces a new method of fabricating diphasic ceramic microstructures with controlled phase dimensionality and anisotropy provided by thin parallel arrays (microlaminae) of 2 thermodynamically-compatible ceramic pastes (boehmite/zirconia). Multiphase alumina/zirconia components were produced from nano-size sol-derived pastes using co-extrusion. The feasibility of forming multiphase aligned fibrilar microstructures using the innovative co-extrusion process developed is shown to be achiaviable if the rheology of the two pastes, drying and sintering shrinkage are both optimised and controlled in order to eliminate the crack formation within the filaments or at the interface. 3rd co-extrusion provides a filament size of about 60–70 μm and these plastically deformable co-extruded filaments in green state are layed up in desired shape mold to produce net shape components. The final pressureless sintered (1400 °C for 2 h) alumina and zirconia microstructures within the co-extruded matrix are very fine (the average grain size of alumina and zirconia are determined to be 1.6 and 0.45 μm, respectively) and pore free. This processing technique allows us to produce damage-tolerant components with the application of zirconia interface during co-extrusion or lay up stages in the final mold.

Acknowledgements

This project is supported by the European Commission under the contract number BRITE- EURAM, BRPR- CT 97- 0609. Project partners; University of Warwick (UK), Morgan Materials Technology, M^2T (UK), Centro de Estudios e Investigaciones, CEIT

(Spain), Ecole des Mines de Paris (France) and Industria de Turbo Propulsores (Spain) are sincerely acknowledged for their contribution. Mr. R. Huzzard is acknowledged for the assistance with rheological measurements.

References

1. Lewis, M. H., Daniel, A. M., Chamberlain, A., Pharaoh, M. W., Cain, G. Microstructure-property relationships in silicate-matrix composites. *J. Microscopy*, 1993, **169**, 109–121.
2. Evans, A. G. and Marshall, D. B., The mechanical behaviour of ceramic matrix composites. *Acta Metall*, 1989, **37**, 2567–2583.
3. Sutherland, S., Plucknett, K. P. and Lewis, M. H., High temperature mechanical and thermal stability of silicate matrix composites. *J. Composites Eng*., 1995, **5**, 1367–1374.
4. Evans, A. G., Domergue, J.-M. and Vagaggini, E., Methodology for relating the tensile constitutive behaviour of ceramic-matrix composites to constituent properties. *J. Am. Ceram. Soc*., 1994, **77**, 1425–1435.
5. Tu, W., Lange, F. F. and Evans, A. G., Concept for damage-tolerant ceramic composite with "strong" interfaces. *J. Am. Ceram. Soc*., 1996, **79**, 417–424.
6. Shannon, T. and Blackburn, S., The production of alumina/zirconia laminated composites by co-extrusion. *Ceramic Engineering and Science Proceedings*, 1995, **16**, 1115–1120.
7. Liang, Z. and Blackburn, S., Co-extrusion of multilayered tubes. In *Proceedings of The Better Ceramics Through Processing*, ed. J. Yeomans and J. Binner. The Institute of Materials, London, 1998, pp. 109–115.
8. Hoy, W., Barda, A., Griffith, M. and Halloran, J. W., Microfabrication of ceramics by co-extrusion. *J. Am. Ceram. Soc*., 1998, **81**, 152–158.
9. Crumm, A. T. and Halloran, J. W., Fabrication of microconfigured multicomponent ceramics. *J. Am. Ceram. Soc*., 1998, **81**, 1053–1057.
10. Chen, Z., Ikeda, K., Murakami, T. and Takeda, T., Extrusion of metal-ceramic composite pipes. *J. Am. Ceram. Soc*., 2000, **83**, 1081–1086.
11. Kaya, C. and Butler, E. G., Plastic forming and microstructural development of α-alumina ceramics from highly compacted green bodies using extrusion. *J. Eur. Ceram. Soc*., 2002, **22**, 1917–1926.
12. Kaya, C., Butler, E. G. and Lewis, M. H., Microstructurally controlled mullite ceramics from monophasic and diphasic sol-derived pastes. *J. Mater. Sci*. (in press).
13. Kaya, C. and Butler, E. G., Innovative processing of multiphase high temperature ceramics, *Mid-term report to European Commission*, Conract no: BRPR-CT97–069, December 1999.
14. Kaya, C., Butler, E. G. and Lewis, M. H., unpublished work.
15. Clegg, W. C, Kendall, C, Alford, N.M, Button, T.W. and Birchall, J.D., *A simple way to make tough ceramics*. *Nature*, 1990, **347**, 455–457.
16. Kaya, C. and Butler, E. G., Innovative processing of multiphase high temperature ceramics, *Final report to European Commission*, Conract no: BRPR-CT97–069, December 2001.
17. Kaya, C., *Processing and Properties of Alumina Fibre-Reinforced Mullite Ceramic Matrix Composites*. PhD Thesis, The University of Birmingham, June 1999.
18. Huzzard, R. J. and Blackburn, S., Influence of solids loading on aqueous injection moulding paste. *Brit. Ceram. Trans*, 1999, **98**, 49–56.
19. Draper, O., Blackburn, S., Dolman, G., Smalley, K. and Griffiths, A., A comparison of paste rheology and extrudate strength with respect to binder formulation and forming technique. *Mater. Processing Tech*., 1999, **92–93**, 141–146.
20. Huzzard, R. J. and Blackburn, S., Slip flow in concentarted alumina suspensions. *Powder Technology*, 1998, **97**, 118–123.
21. Benbow, J. and Bridgwater, J., *Paste Flow and Extrusion*. Clarendon Press, Oxford, 1993.
22. Kaya, C., Butler, E. G. and Lewis, M. H., Processing and characterisation of mullite (Nextel 720™) fibre-reinforced mullite matrix composites from hydrothermally processed mullite precursors. In *High Temperature Ceramic Matrix Composites (HT-CMC 4)*, ed. W. Krenkel, R. Naslain and H. Schneider. Wiley-VCH, Weinheim, Germany, 2001, pp. 639–644.
23. Wendorff, J., Janssen, R. and Claussen, N., Platinum as a weak interphase for fiber-reinforced oxide-matrix composites. *J. Am. Ceram. Soc*., 1998, **81**, 2738–2740.
24. Kaya, C., Kaya, F., Boccaccini, A. R. and Chawla, K. K., Fabrication and characterisation of ni-coated carbon fibre-reinforced alumina ceramic matrix composites using electrophoretic deposition. *Acta Materialia*, 2001, **49**, 1189–1197.
25. Mendelson, M. I., Average grain size in polycrystalline ceramics. *J. Am. Ceram. Soc*., 1969, **52**, 443–446.
26. Whorlow, R. W., *Rheological Techniques*. Ellis Horwood, London, 1992.